Electronic Supplementary Material (ESI) for Journal of Materials Chemistry A.

Supporting Information

Pure spin current generated in thermal driven molecular magnetic junctions: a promising mechanism for thermoelectric conversion

Dan Wu[a], Xuan-Hao Cao[a], Shi-Zhang Chen[a], Li-Ming Tang[a], Ye-Xin Feng[a], Ke-Qiu Chen*[a], Wu-Xing Zhou*[b]

[a] *Department of Applied Physics, School of Physics and Electronics, Hunan University, Changsha 410082, China*
E-mail: keqiuchen@hnu.edu.cn (K. Q. Chen)
[b] *School of materials Science and Engineering, Hunan University of Science and Technology, Xiangtan 411201, China*
E-mail: wuxingzhou@hnu.edu.cn (W. X. Zhou)

1. Effect of headgroup-substrate binding geometries on transport

The $CoCp_2$-Ac-$CoCp_2$-based molecule junction is formed by $CoCp_2$-Ac-$CoCp_2$ molecule chemisorbed on Au (111) surface via sulphur group, as shown in Fig. S1. Using the scanning tunneling microscope (STM) or atomic force microscope (AFM) break junction techniques, there are three common contact point geometries of molecule and electrodes,[1, 2] e.g. the contacts of top-hollow, hollow-hollow, and top-top. The sulphur atoms on both of ends linking to the 3-Au atoms hollow sites of the Au (111) surface is denoted hollow-hollow geometry, which is shown in Fig. S1 (a) (studied in

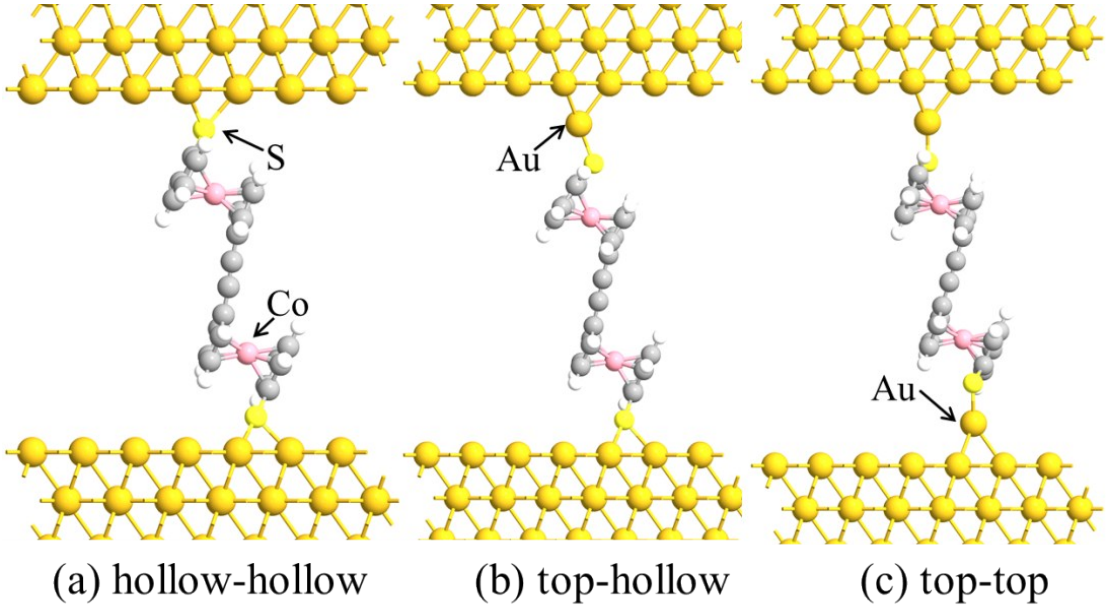

Fig. S1 Possible contact configurations of molecule and leads for (a) hollow-hollow, (b) top-hollow, and (c) top-top.

the text). The top-top geometry is formed by two sulphur atoms linking to two top sites of the Au (111) surface, as shown in Fig. S1 (c). The geometry of Fig. S1 (b) is denoted top-hollow. These configurations have effect on the electron transport originating from the changing of binding force between electrodes and molecule or the number of involvement electron.

Fig. S2 shows electron transmission spectra for contact geometries of hollow-hollow (dashed line), top-hollow (magenta and yellow) and top-top (black and olive). As

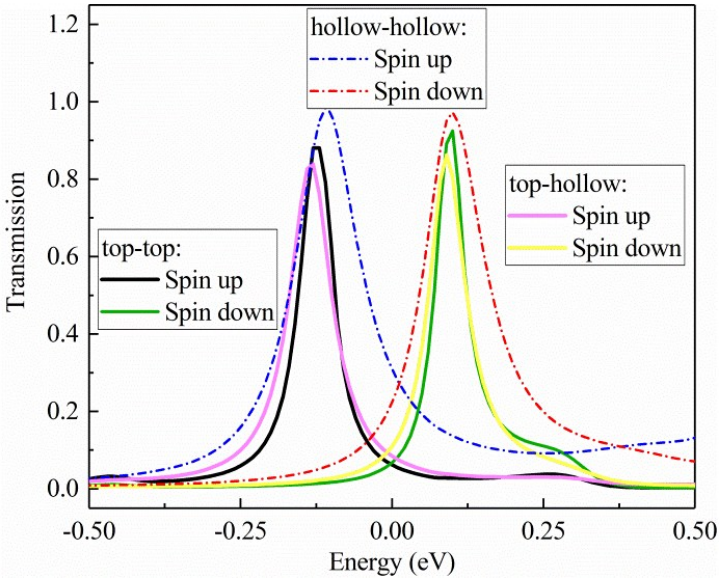

Fig. S2 The transmission spectra for hollow-hollow, top-hollow and top-top contact geometries versus energy.

compared with the electron transmission spectra of hollow-hollow configuration, top-hollow and top-top configuration show similar spin up and spin down transmission peak near Fermi level, while the broadening of transmission coefficient becomes narrow. These results suggest that the electron transport performance of hollow-hollow structure is superior to the other contact geometries. However, a common feature for top-hollow and top-top configurations is that the transmission

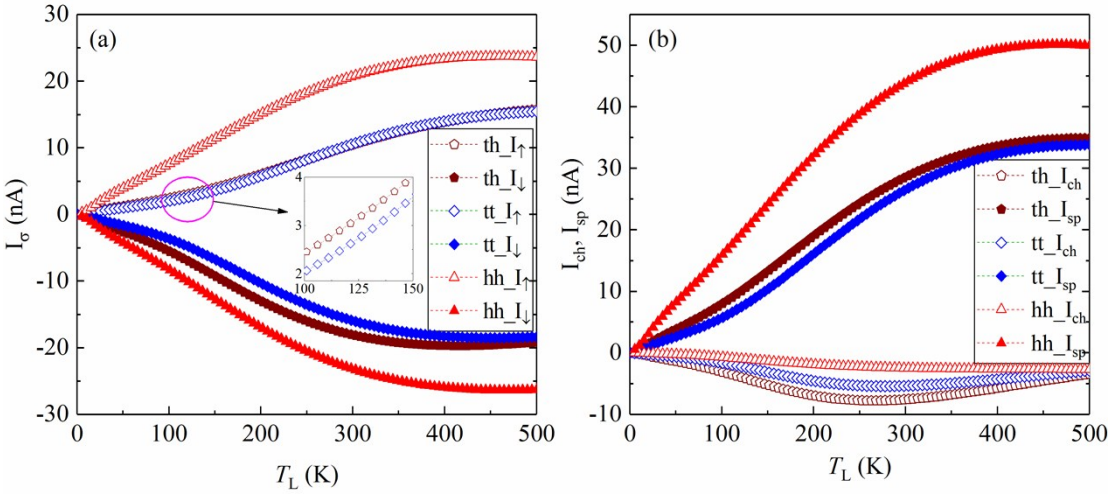

Fig. S3 (a) The thermal-induced spin-up current ($I_\uparrow$) and spin-down current ($I_\downarrow$) and (b) the charge current (I_{ch}) and the spin current (I_{sp}) versus T_L at ΔT=20K for top-hollow, top-top and hollow-hollow contact configuration in Au-$CoCp_2$-Ac-$CoCp_2$ system, respectively. The th_ $I_\uparrow$ and th_ I_{ch} represent the spin-up current and charge current of top-hollow contact configuration.

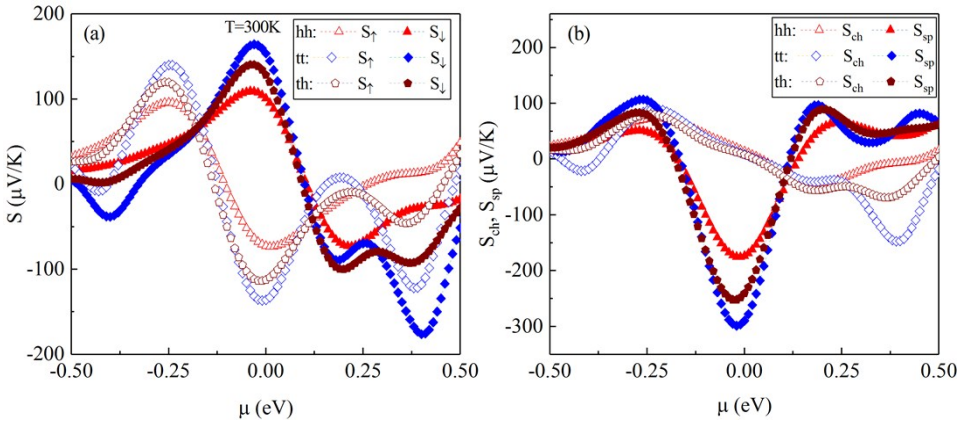

Fig. S4 The spin-up Seebeck coefficient ($S_{\uparrow}$), spin-down Seebeck coefficient ($S_{\downarrow}$), charge Seebeck coefficient (S_{ch}), and spin-dependent Seebeck coefficient (S_{sp}) as function of chemical potential at room temperatures top-hollow, top-top and hollow-hollow contact configuration in Au-$CoCp_2$-Ac-$CoCp_2$ system, respectively.

function of spin up and spin down are almost symmetrical about Fermi level. It demonstrates that a pure spin current may be obtained.

When a temperature difference is applied across the junction, the thermal spin-polarized current and spin-dependent Seebeck coefficient are displayed in Fig. S3 and Fig. S4. The value of spin current in hollow-hollow structure is larger than that in top-hollow and top-top structure, which is depend on the broadening of transmission coefficient near Fermi level. In addition, the th_$I_{\uparrow}$ and th_$I_{\downarrow}$ (tt_$I_{\uparrow}$ and tt_$I_{\downarrow}$) are approximately symmetrical about zero current axis at some temperature regions, and a pure spin current can be obtained at the corresponding temperature regions (blue rhombus and wine pentagon in Fig. S3 (b)). Fig. S4 shows the spin-dependent Seebeck coefficient for hollow-hollow, top-hollow and top-top contact configurations in Au-CoCp2-Ac-CoCp2 system, respectively. Because of the dependence of S_{σ} on the value and the slop of $\tau_{\sigma}(\varepsilon_f)$ (ε_f denotes Fermi level), the S_{σ} of top-hollow and top-top structure are larger than that of hollow-hollow structure. Besides, the S_{ch} of top-hollow and top-top structure approaches zero at chemical potential region [-0.25 eV, 0.25 eV], which indicates that a pure thermopower may be achieved.

2. Effect of the coupling strength between lead and molecule on transport

The different coupling strength between lead and molecule are also common in

experiment.[3, 4] The strong coupling systems, where $CoCp_2$-Ac-$CoCp_2$ molecule is chemisorbed on Au (111) surface via Au-S hybridization with covalent bonds, are shown in the C1 (studied in text part) and C2 structure of Fig. S5. The weak coupling system, which is formed by molecule and Au surface with no-covalent bonds, is shown in C3 structure of Fig. S5. The transmission spectrum of C2 configuration (black and olive in Fig. S5) shows very similar characteristics at the energy region [-0.5, 0.5] as compared with C1 configuration (dash line in Fig. S5). However, for C3

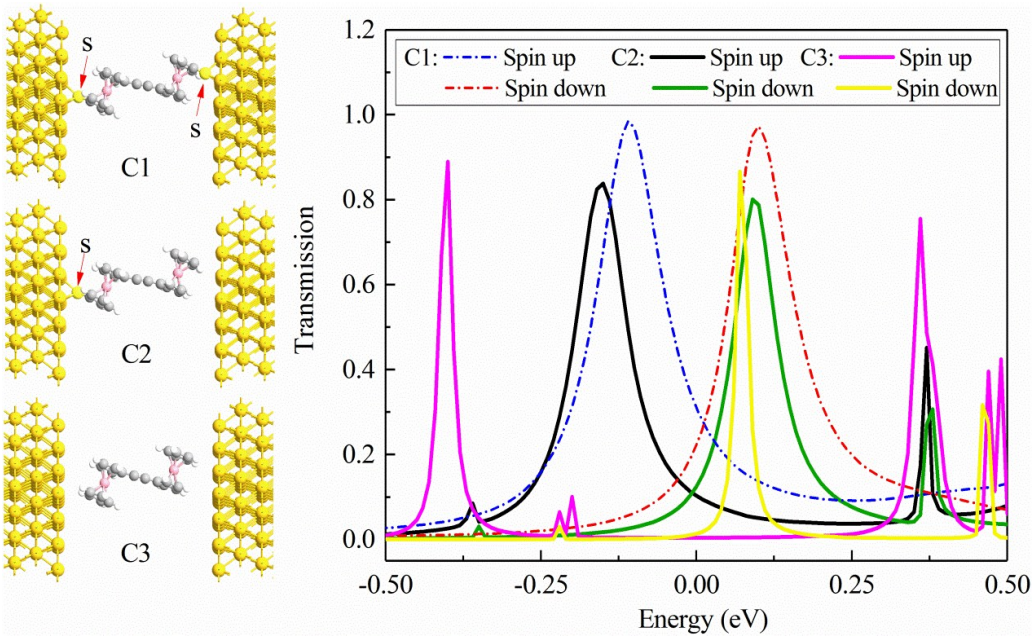

Fig. S5 The electronic transmission spectra of C1, C2, and C3 contact configuration in Au-$CoCp_2$-Ac-$CoCp_2$ system. The contact configuration of C1: 2S atom bonded with two Au surface (strong coupling); C2: 1S atom bonded with left-Au surface (strong coupling); C3: 0S atom bonded with Au surface (weak coupling).

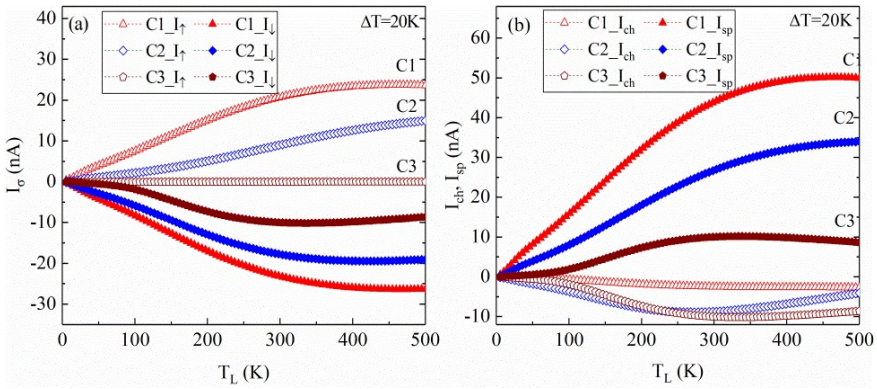

Fig. S6 (a) The thermal driven spin-up current ($I_{\uparrow}$) and spin-down current ($I_{\downarrow}$) and (b) the charge current (I_{ch}) and the spin current (I_{sp}) versus T_L at ΔT=20K for C1, C2 and C3 contact configuration

in Au-$CoCp_2$-Ac-$CoCp_2$ system, respectively.

junction, the transmission peak contributed by HOMO (highest occupied molecular orbital) level of spin up (magenta in Fig. S5) and LUMO (lowest unoccupied molecular orbital) level of spin down (yellow in Fig. S5) becomes narrow, and the highest peak dominated by HOMO level is far away from Fermi level. A reasonable explanation is that the strong interaction of leads and molecule broadens the HOMO and LUMO level, causing significant overlapping of both electronic states. In contrast, the interaction of leads and molecule becomes weak, and the energy barrier of HOMO and LUMO increases, which results in the electron transport being blocked due to mismatch of energy-level.[5]

Fig. S6 shows thermal spin-polarized current for C1, C2 and C3 versus T_L at ΔT=20K. The $I_{\uparrow}$ and $I_{\downarrow}$ of C2 are not completely equal at some temperature regions, causing the existence simultaneously of I_{ch} and I_{sp}. While $I_{\uparrow}$of C3 is blocked in all temperature regions, resulting in a perfect spin filtering effect. Fig. S7 shows the spin-dependent Seebeck coefficient for C1, C2 and C3 versus chemical potential at room temperature. The calculation shows the S_{σ} of C3 is larger than that of C1 and C2, originating from the steep slope of $\tau_{\sigma}(\varepsilon_f)$.

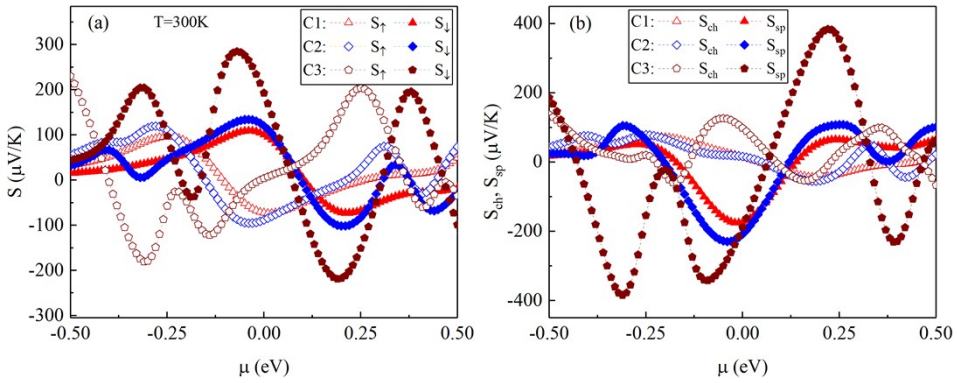

Fig. S7 The spin-up Seebeck coefficient ($S_{\uparrow}$), spin-down Seebeck coefficient ($S_{\downarrow}$), charge Seebeck coefficient (S_{ch}), and spin-dependent Seebeck coefficient (S_{sp}) as function of chemical potential at room temperatures for Au-$CoCp_2$-Ac-$CoCp_2$ system, respectively.

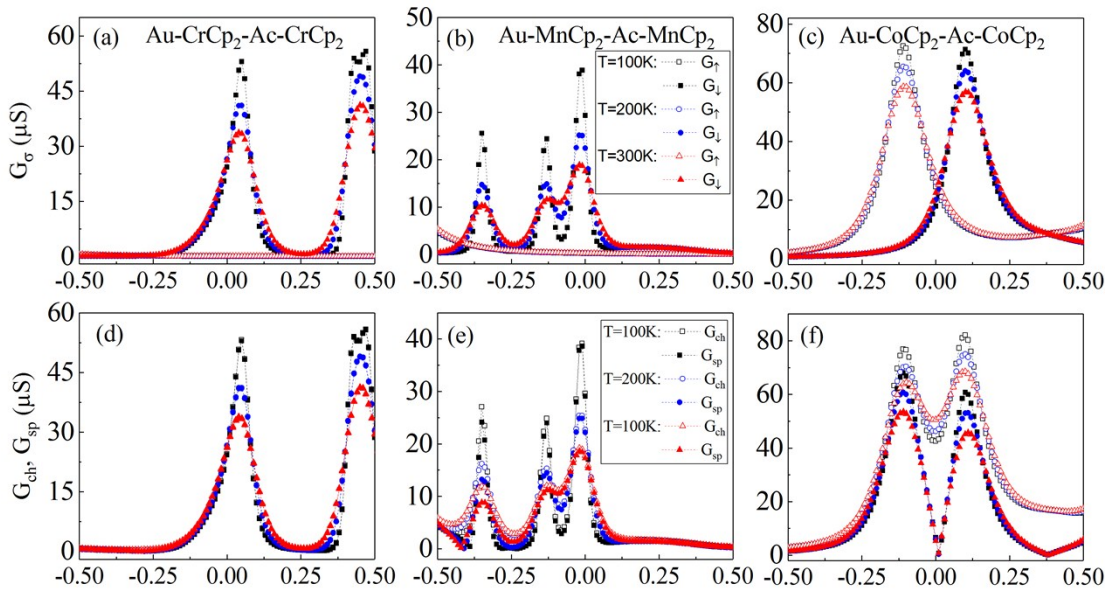

Fig. S8 (a)-(c) spin-polarized conductance (d)-(f) charge and spin-dependent conductance as function of chemical potential at different temperature for Au-$CrCp_2$-Ac-$CrCp_2$, Au-$MnCp_2$-Ac-$MnCp_2$ and Au-$CoCp_2$-Ac-$CoCp_2$, respectively.

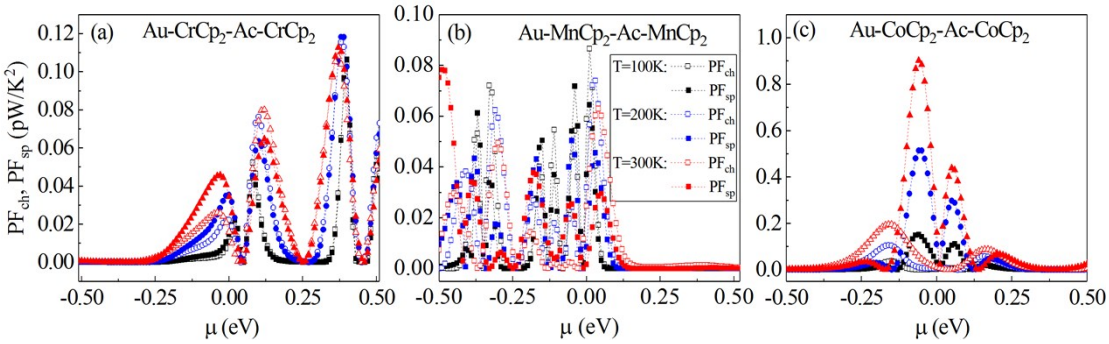

Fig. S9 (a)-(c) Charge power factor (PF_{ch}) and spin-dependent power factor (PF_{sp}) as function of chemical potential at different temperature for Au-$CrCp_2$-Ac-$CrCp_2$, Au-$MnCp_2$-Ac-$MnCp_2$ and Au-$CoCp_2$-Ac-$CoCp_2$, respectively.

References

1. C. M. Kim and J. Bechhoefer, *J.Chem. Phys*, 2013, **138**, 014707.
2. M. Frei, S. V. Aradhya, M. S. Hybertsen and L. Venkataraman, *J. Am. Chem. Soc.*, 2012, **134**, 4003-4006.
3. G. Kuang, S.-Z. Chen, W. Wang, T. Lin, K. Chen, X. Shang, P. N. Liu and N. Lin, *J. Am. Chem. Soc.*, 2016, **138**, 11140-11143.
4. L. Yuan, L. Wang, A. R. Garrigues, L. Jiang, H. V. Annadata, M. A. Antonana, E. Barco and C. A. Nijhuis, *Nat. Nanotechnol.*, 2018, **13**, 322.
5. L. Bogani and W. Wernsdorfer, *Nat*. *Mater*., 2008, **7**, 179.